Since January 2020 Elsevier has created a COVID-19 resource centre with free information in English and Mandarin on the novel coronavirus COVID-19. The COVID-19 resource centre is hosted on Elsevier Connect, the company's public news and information website.

International Journal of Infectious Diseases 103 (2021) 517–524

Contents lists available at ScienceDirect

International Journal of Infectious Diseases

journal homepage: www.elsevier.com/locate/ijid

Simultaneous detection and differentiation of SARS-CoV-2, influenza A virus and influenza B virus by one-step quadruplex real-time RT-PCR in patients with clinical manifestations

Minjun Ni[a], Hengyi Xu[b], Jie Luo[a], Wei Liu[c], Donggen Zhou[a,c,*]

[a] Ningbo International Travel Healthcare Centre, Ningbo, People's Republic of China
[b] State Key Laboratory of Food Science and Technology, Nanchang University, Nanchang, People's Republic of China
[c] Nanchang International Travel Healthcare Centre, Nanchang, People's Republic of China

ARTICLE INFO

Article history:
Received 24 October 2020
Received in revised form 2 December 2020
Accepted 10 December 2020

Keywords:
SARS-CoV-2
Influenza A virus
Influenza B virus
Differentiation
Quadruplex
Co-infection

ABSTRACT

Objective: To develop a novel quadruplex real-time reverse transcription polymerase chain reaction (rRT-PCR) assay for the diagnosis of severe acute respiratory syndrome coronavirus-2 (SARS-CoV-2) infection, differential diagnosis and detection of co-infections.
Methods: A one-step quadruplex rRT-PCR assay was developed for simultaneous detection and differentiation of SARS-CoV-2 ORF1ab and N genes, influenza A virus (hIAV) and influenza B virus (hIBV).
Results: The quadruplex rRT-PCR assay had good sensitivity and specificity. Correlation coefficients and amplification efficiencies of all singleplex and quadruplex rRT-PCR reactions were within acceptable ranges. The 95% lower limits of detection for plasmid standards and positive nucleic acid extracts of the quadruplex rRT-PCR assay were 57.38–95.11 copies/μL and 114.65–154.25 copies/μL, respectively. Excellent results were attained for inter- and intra-assay reproducibility. Among these clinical samples, only four samples showed results inconsistent with the singleplex rRT-PCR assays.
Conclusions: To the authors' knowledge, this is the first study to report a quadruplex rRT-PCR assay for the detection of two SARS-CoV-2 genes, hIAV and hIBV with perfect clinical performance.

Introduction

Severe acute respiratory syndrome coronavirus-2 (SARS-CoV-2), named by the International Committee on Taxonomy of Viruses (Valencia, 2020), was first recorded in Wuhan, China in December 2019, and has since spread worldwide; a pandemic was declared by the World Health Organization (WHO) in March 2020 (Huang et al., 2020). As of 27 September 2020, SARS-CoV-2 has caused nearly 32 million infections and 991,000 deaths worldwide (WHO, 2020a). This new coronavirus belongs to the genus Betacoronavirus and subgenus Sarbecovirus (lineage B), with its genome sharing more than 96% similarity with the genome of bat coronavirus (BatCoV RaTG13).

Infection with SARS-CoV-2 causes coronavirus disease 2019 (COVID-19), which is mainly manifested by respiratory symptoms including fever, cough, dyspnoea and fatigue (Zheng, 2020). For patients who test positive for SARS-CoV-2, blood tests usually show leukopenia and lymphopenia, and computed tomography scans show bilateral multi-lobar ground-glass opacities in the lungs (Zheng, 2020). The clinical manifestations of SARS-CoV-2 range from asymptomatic carriers to acute respiratory distress syndrome. Most individuals exhibit mild symptoms or remain asymptomatic (Wang et al., 2020). As the low viral load of SARS-CoV-2 is very weakly positive or single-target positive, an ultrasensitive assay is required for its detection. Real-time reverse transcription polymerase chain reaction (rRT-PCR) assays have high sensitivity, good specificity and good repeatability (Lai et al., 2020), and are recommended by WHO for the detection and confirmation of SARS-CoV-2 (Okela et al., 2010).

The clinical symptoms of SARS-CoV-2 are very similar to those caused by influenza A virus (hIAV) and influenza B virus (hIBV); specific and sensitive assays are required for effective differentiation of these two influenza viruses (Valencia, 2020) from SARS-CoV-2 and other influenza viruses to enable precise treatment, and prevention and control. Generally, virus isolation based on cell culture is the 'gold standard' for the diagnosis of viral diseases, but this is time consuming and complicated (WHO, 2020b).

* Corresponding author at; Ningbo International Travel Healthcare Centre, 315012 Ningbo, People's Republic of China.
E-mail address: Dongdong1004@163.com (D. Zhou).

https://doi.org/10.1016/j.ijid.2020.12.027

Particularly when clinical symptoms are atypical and may not be pathogen specific, time-consuming virus-specific assays are needed for accurate diagnosis of the target pathogen (Wilkesmann et al., 2006). As such, there is a need for the development of a rapid assay for simultaneous detection of SARS-CoV-2 and influenza virus.

Many PCR and multiplex rPCR assays have been developed for the effective identification and differentiation of influenza viruses and other respiratory viruses (Coiras et al., 2003; Williams et al., 2004; Hindiyeh et al., 2005; Fang et al., 2011). To the authors' knowledge, no multiplex rRT-PCR assays have been reported for simultaneous detection of SARS-CoV-2, hIAV and hIBV. As such, the authors developed a quadruplex rRT-PCR assay that can simultaneously detect and differentiate between SARS-CoV-2 ORF1ab and N genes, hIAV and hIBV in one tube from different clinical specimens from the respiratory tract, such as nasopharyngeal swabs, oropharyngeal swabs and sputum.

Materials and methods

Primer and probe design

The complete genome of SARS-CoV-2 was downloaded from the GISAID database, and hIAV and hIBV sequences were downloaded from the GenBank database. These sequences were aligned and analysed to identify the conserved segments of these four targets that can cover all isolates as primer and probe candidates for rRT-PCR using MEGA7. Primer Premier 5.0 was used to design four target-specific primers and probes (Table 1). ClustalW2.0 (http://www.ebi.ac.uk/Tools/msa/clustalw2/) was used to align the sequences. The numbers of SARS-CoV-2 genome, influenza A virus matrix protein (M) gene and influenza B virus neuraminidase (NA) gene sequences used for alignment were 440, 312 and 325, respectively.

The four sets of primer and probe sequences designed were analysed using the BLAST tool. These primers and probes were synthesized by Shanghai Sangon Biological Engineering Co., Ltd (Shanghai, People's Republic of China) and purified by high-performance liquid chromatography.

Preparation of viral RNA in-vitro transcript standards

The T7 RNA polymerase promoter sequence was added to the 5′ ends of the four designed target segment sequences to form artificial constructs, and then sent to Shanghai Sangon Biological Engineering Co., Ltd for double-stranded DNA synthesis. Double-stranded DNA constructs were transcribed *in vitro* with T7 RNA polymerase and subsequently digested with DNase I. The digested products were purified using an RNA purification kit, and four RNA plasmid standards were prepared. Following purification, the copy number of each RNA plasmid standard was determined using a nucleic acid analyser, and the RNA plasmid standard with the determined copy number was serially diluted with TE buffer.

Species-specific sample panel

The species-specific sample panel included the following samples: human coronavirus 229E (n = 6), human coronavirus NL63 (n = 3), human coronavirus OC43 (n = 4), human coronavirus HKU1 (n = 3), parainfluenza virus type 1/2/3 (n = 5), adenovirus (n = 8), respiratory syncytial virus group A/group B (n = 5), human metapneumovirus (n = 3), human bocavirus (n = 4) and rhinovirus (n = 8). All of these samples tested positive on their respective rRT-PCR assays and were kept at Ningbo International Travel Healthcare Centre (Ningbo ITHC, Ningbo, People's Republic of China). *Mycoplasma pneumoniae* (n = 2), *Chlamydia pneumoniae* (n = 3), *Legionella* sp. (n = 2), *Bordetella pertussis* (n = 1), *Klebsiella pneumoniae* (n = 5) and *Mycobacterium tuberculosis* (n = 1) were kindly provided by Ningbo Centre for Disease Prevention and Control (Ningbo CDC, Ningbo, People's Republic of China). SARS-CoV (n = 1) was an artificial pseudovirus provided by the National Centre for Clinical Laboratories (NCCL, Beijing, People's Republic of China), and Middle East respiratory syndrome virus (n = 3) was an inactivated EQA sample provided by Quality Control for Molecular Diagnostics (QCMD, Glasgow, UK).

Subtype-specific sample panel

Subtype-specific sample panels included the following samples: SARS-CoV-2 national reference (n = 1), influenza A (H1N1) pdm09 virus (n = 18), influenza A virus (H3N2) (n = 21), influenza A virus (H7N9) (n = 1), influenza A virus (H5N1) (n = 1), influenza B virus Yamagata lineage (n = 6) and influenza B virus Victoria lineage (n = 9). Influenza A (H1N1) pdm09 virus and influenza A virus (H3N2) tested positive for their respective rRT-PCR assays and were kept at Ningbo ITHC. The SARS-CoV-2 national reference was purchased from NCCL. Influenza A virus (H7N9), influenza A virus (H5N1) and the Yamagata and Victoria strains of influenza B virus were provided by Ningbo CDC.

RNA extraction

Viral RNA was extracted and purified with a GenePure Pro automatic nucleic acid extraction and purification system (NPA-32 P; Hangzhou Bioer Technology Co., Ltd, Hangzhou, People's Republic of China) using a MagaBio Plus Viral DNA/RNA Purification Kit II (BSC71S1B; Hangzhou Bioer Technology Co., Ltd) in accordance with the manufacturer's instructions. The extracted RNA was frozen and stored at −80 °C.

Table 1
Primers/probes used in this work.

Target	Oligo	Primer/probe sequence (5′–3′)	Target gene	Length (nt)	Amplicon size (bp)
hIAV	Fr	GACCRATCCTGTCACCTCTGAC	Matrix protein (M)	22	89
	Rv	AGGGCATTYTGGACAAAKCGTCTA		24	
	Probe	ROX-TGCAGTCCTCGCTCACTGGGCACG-BHQ2		24	
hIBV	Fr	GGGATAGARATGGTACATGATGGTG	Neuraminidase (NA)	25	93
	Rv	TGTGACAGTGTCCCACAGCAG		21	
	Probe	CY5-ACTTGGCACTCAGCRGCAACAGCC-BHQ3		24	
SARS-CoV-2 N gene	Fr	CCCCAAGGTTTACCCAATAAT	Nucleocapsid (N)	21	87
	Rv	GGTCTTCCTTGCCATGTTGA		20	
	Probe	VIC-CTGCGTCTTGGTTCACCGCTCTCAC-BHQ1		25	
SARS-CoV-2 ORF1ab gene	Fr	CATACACTCGCTATGTCGATAAC	Open reading frame 1ab (ORF1ab)	23	103
	Rv	AGTGTCAATAAAGTCCAGTTGTTC		24	
	Probe	FAM-CTTCTGTGGCCCTGATGGCTACCCTC-BHQ1		26	

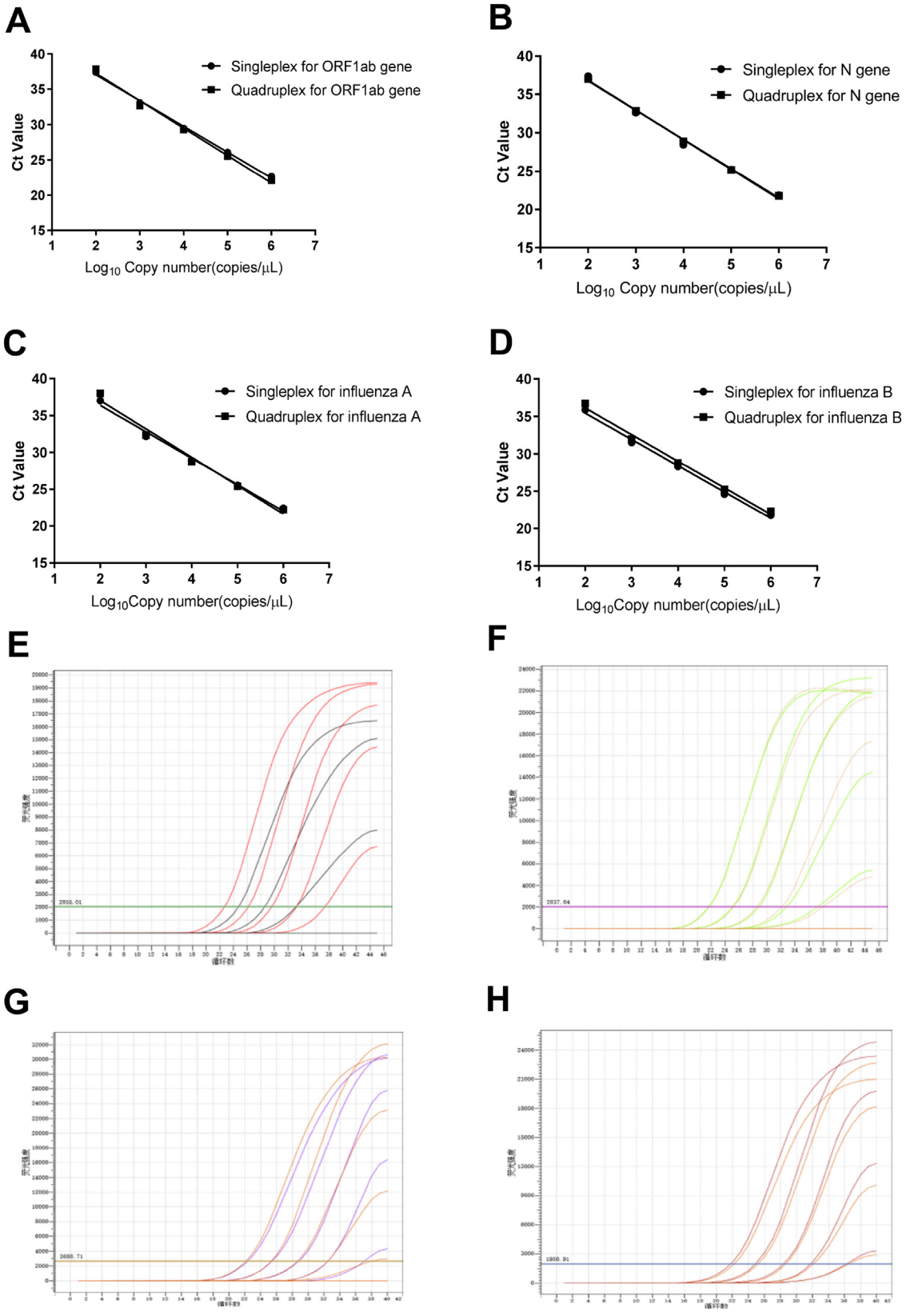

Figure 1. Comparative standard curves and amplification plots of the quadruplex and singleplex real-time reverse transcription polymerase chain reaction assays using 10-fold serially diluted plasmid standards of the ORF1ab gene, N gene, influenza A virus (hIAV) and influenza B virus (hIBV) ranging from 106 to 102 copies/μL. (A, E) Standard curves and amplification plots of the ORF1ab gene. (B, F) Standard curves and amplification plots of the N gene. (C, G) Standard curves and amplification plots of hIAV. (D, H) Standard curves and amplification plots of hIBV.

Singleplex and quadruplex rRT-PCR assays

All rRT-PCR assays were performed on a LineGene 9600 Plus fluorescent quantitative PCR detection system (FQD-96A; Hangzhou Bioer Technology Co., Ltd). A BioRT Real-time RT-PCR Kit II (BSB66; Hangzhou Bioer Technology Co., Ltd) for singleplex or multiplex rRT-PCR assays was used for detection. The rRT-PCR assays were performed using a final volume containing 12.5 μL of 2×RT-PCR solution, 1.3 μL of enzyme complex, 1.8 μL of primer complex compound, 2.05 μL of probe complex and 5 μL of RNA template, made up to a total volume of 25 μL with nuclease-free water. The reactions were incubated at 50 °C for 10 min, followed by 95 °C for 1 min and 45 cycles of 95 °C for 15 s and 60 °C for 45 s.

Standard curve of singleplex and quadruplex rRT-PCR assays

The four RNA plasmid standards were mixed equally and serially diluted 10-fold with TE buffer to five dilutions ($1 \times 10^6 \sim 1 \times 10^2$ copies/μL) for each target. The quadruplex rRT-PCR assay and the corresponding singleplex rRT-PCR assays were used to detect these RNA plasmid standard dilutions. Cycle threshold (Ct) values were plotted against $\log_{10}$ plasmid concentrations to establish a standard curve, and linear regression analysis was performed for the four targets, allowing determination of the correlation coefficient (R^2). The amplification efficiencies (E) of the reactions were calculated from the curves using the equation $E = (10^{(-1/\text{slope})} - 1) \times 100\%$.

Analytical sensitivity of singleplex and quadruplex rRT-PCR assays

Analytical sensitivity of the singleplex and quadruplex rRT-PCR assays was determined using RNA plasmid standards and positive nucleic acid extracts, respectively. For RNA plasmid standards, four RNA plasmid standards were mixed equally and serially diluted 10-fold with TE buffer to 1000 copies/μL, 500 copies/μL, 250 copies/μL, 125 copies/μL, 62.5 copies/μL, 31.3 copies/μL and 15.6 copies/μL. Each dilution was tested by the one-step quadruplex rRT-PCR assay and its corresponding singleplex assays in 20 replicates, and the lower limit of detection (LLOD) was defined as the concentration of copies/μL of the lowest dilution that could be detected with ≥95% probability and determined by probit analysis. For the positive nucleic acid extract of SARS-CoV-2, the concentration was calibrated by digital PCR to be 3×10^5 copies/μL, and the positive nucleic acid extract was serially diluted to 300 copies/μL, 150 copies/μL, 75 copies/μL, 62.5 copies/μL and 31.3 copies/μL. For the positive nucleic acid extracts of hIAV and hIBV, the concentrations were calibrated by digital PCR to be 1.5×10^5 copies (equivalent genomes)/μL and 2×10^5 copies (equivalent genomes)/μL, respectively, and serially diluted 1000-fold, 2000-fold and 4000-fold. Each dilution was tested by the one-step quadruplex rRT-PCR assay and its corresponding singleplex assays in 20 replicates, and LLOD was defined as the concentration of copies/μL of the lowest dilution that could be detected with ≥95% probability and determined by probit analysis.

Inter- and intra-assay reproducibility

Variability of the quadruplex rRT-PCR assay was assessed by detecting three concentrations (10^6, 10^4 and 10^2 copies/μL) of each target RNA plasmid standard. For intra-assay repeatability, each dilution was analysed in triplicate in one reaction. For interassay reproducibility, each dilution was analysed in three independent reactions performed by different users on separate days. Variability of the Ct value was assessed by variable analysis.

Specificity of quadruplex rRT-PCR assay

Specificity of the quadruplex rRT-PCR assay was evaluated by testing the species-specific sample panel (n = 65) and subtype-specific sample panel (n = 57).

Clinical evaluation

Clinical performance of the quadruplex rRT-PCR assay was evaluated by testing clinical specimens of different types. Upper respiratory tract samples (nasopharyngeal swabs and oropharyngeal swabs) were collected from a patient and placed immediately in a disposable virus sampling tube containing 3 mL of virus transport medium. Lower respiratory tract samples (sputum) from a patient were preprocessed with an equal volume of sputum liquidation buffer before nucleic acid extraction.

Statistical analysis

Basic statistical analysis, including mean, standard deviation and coefficient of variation of the mean Ct value, were calculated using Excel (Microsoft Corp., Redmond, WA, USA). Probit analysis was carried out using SPSS Version 22 (IBM Corp., Armonk, NY, USA). Bland–Altman agreement analysis was used to highlight the correlation between the Ct value of the quadruplex rRT-PCR assay and the corresponding singleplex rRT-PCR assay results using GraphPad (GraphPad Software Inc., La Jolla, CA, USA). Linear regression analysis was also performed using GraphPad.

Results

Standard curve of quadruplex rRT-PCR assay

To determine the dynamic range of the one-step quadruplex rRT-PCR assay, each RNA plasmid standard was serially diluted 10-fold and tested to obtain standard curves and amplification plots of the quadruplex and singleplex rRT-PCR assays (Figure 1).

There was no appreciable variation in the mean Ct values of the singleplex and quadruplex rRT-PCR assays for the ORF1ab gene, N gene, hIAV or hIBV ($p < 0.05$ for all), indicating that these two assays had good consistency. Therefore, both assays may be regarded as equally sensitive for diagnostic purposes.

R^2, E and slopes of the standard curves of the ORF1ab gene, N gene, hIAV and hIBV in the quadruplex and singleplex rRT-PCR assays were calculated and are listed in Table 2.

Table 2
Summary of linear regression results.

	Singleplex rRT-PCR assay				Quadruplex rRT-PCR assay			
	ORF1ab gene	N gene	hIAV	hIBV	ORF1ab gene	N gene	hIAV	hIBV
R^2	0.9974	0.9955	0.9918	0.9953	0.9928	0.9964	0.9846	0.9927
E	93.7%	98.6%	90%	92.6%	86.1%	88.2%	86.9%	90.6%
Slope	−3.483	−3.356	−3.587	−3.512	−3.707	−3.641	−3.682	−3.57

rRT-PCR, real-time reverse transcription polymerase chain reaction; R^2, correlation coefficient; E, amplification efficiency.

For the quadruplex rRT-PCR assay, *E* of each detection target should be 80–120% (corresponding to the slope of the standard curve between -3.9 and -2.9), and R^2 should be ≥0.98 (Broeders et al., 2014). R^2 values for the four detection targets of the quadruplex rRT-PCR assay were all ≥0.9846, and *E* was between 86.1% and 90.6%. This result is acceptable for multiple screening methods, and also indicated that using all four sets of primers and probes in the quadruplex amplification system did not lead to significant cross-interference.

Analysis of sensitivity of quadruplex rRT-PCR assay

LLOD was determined for each target in the quadruplex rRT-PCR assay by probit analysis using RNA plasmid standard dilutions and positive nucleic acid extract dilutions (Table 3).

For the RNA plasmid standards, LLOD was calculated to be 49.96 copies/μL for ORF1ab, 47.56 copies/μL for N, 73.14 copies/μL for hIAV, and 55.20 copies/μL for hIBV. For the nucleic acid extracts, LLOD was calculated to be 100.82 copies/μL for ORF1ab, 100.4 copies/μL for N, 119.74 copies/μL for hIAV, and 114.65 copies/μL for hIBV. LLOD was highest for the N gene, and its detection was the most sensitive among the four targets (Figure 2).

Sensitivities of the singleplex and quadruplex rRT-PCR assays did not differ significantly ($p < 0.05$). The results showed that these two assays have high sensitivity, supporting their exploration as potential diagnostic tools.

Inter- and intra-assay reproducibility of quadruplex rRT-PCR assay

Reproducibility of the quadruplex rRT-PCR assay was determined by calculating the mean and standard deviation of Ct values. Variable analysis showed that the Ct values of different plasmid concentrations did not differ significantly. The coefficients of variation for intra- and interassay testing ranged from 1.26% to 4.83%, and from 2.84% to 5.32%, respectively. These results show that the quadruplex rRT-PCR assay is accurate and has good repeatability, even for low-concentration samples.

Specificity of quadruplex rRT-PCR assay

Specificity of the quadruplex rRT-PCR assay was verified in two ways. First, the primers and probe sequences were aligned *in silico* with the sequences of SARS-CoV-2, hIAV and hIBV in the GenBank and GISAID databases to ensure that the primers and probes could match the target gene sequence correctly. rRT-PCR assay, but the subtype-specific sample panel had obvious amplification signals (Table 4), suggesting that this assay has good specificity.

Clinical evaluation

In total, 312 clinical specimens, including 110 nasopharyngeal swabs, 186 oropharyngeal swabs and 16 sputum samples, were collected, confirmed by other commercial rRT-PCR kits approved by the National Medical Products Administration (People's Republic of China), and tested using both the quadruplex and singleplex rRT-PCR assays to compare their sensitivity and specificity. The newly established quadruplex rRT-PCR assay was positive in 41.8% (46/110) of the nasopharyngeal swabs for the SARS-CoV-2 ORF1ab gene and 41.8% (46/110) of the nasopharyngeal swabs for the SARS-CoV-2 N gene, positive in 16.1% (30/186) of the throat swabs for the SARS-CoV-2 ORF1ab gene and 17.7% (33/186) of the throat swabs for the SARS-CoV-2 N gene, and positive in 75% (12/16) of the sputum samples for the SARS-CoV-2 ORF1ab gene and N gene. For three samples, the quadruplex rRT-PCR assay had a detectable signal for the SARS-CoV-2 N gene but no signal for the ORF1ab gene, but the singleplex rRT-PCR assay had a dual target signal. These three samples were retested using both the singleplex and quadruplex rRT-PCR assays after re-extraction of nucleic acids, displaying all the signals for the ORF1ab gene and N gene. For one sample, the quadruplex rRT-PCR assay had a detectable signal whereas the singleplex rRT-PCR assay had no signal. This sample was retested using both the singleplex and quadruplex rRT-PCR assays after re-extraction of nucleic acids, and both assays had signals for the ORF1ab gene and N gene. The quadruplex rRT-PCR assay was positive in 30% (33/110) of nasopharyngeal swabs for hIAV and 26.4% (29/110) of nasopharyngeal swabs for hIBV, and was positive in 14.5% (27/186) of oropharyngeal swabs for hIAV and 11.3% (21/186) of oropharyngeal swabs for hIBV (Table 5).

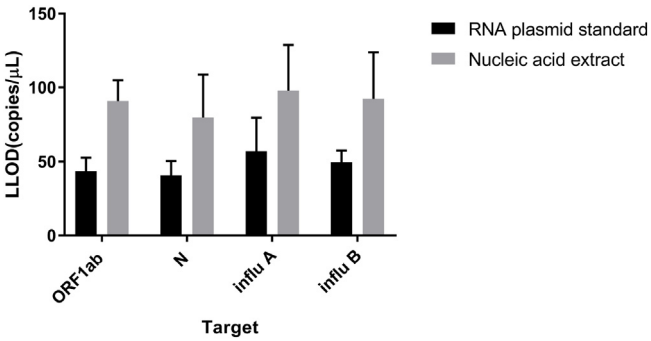

Figure 2. Comparative lower limit of detection (LLOD) plots of the quadruplex and singleplex real-time reverse transcription polymerase chain reaction assays using serially diluted plasmid standards and nucleic acid extracts for the ORF1ab gene, N gene, human influenza A (influ A) and human influenza B (influ B).

Briefly, the distribution frequencies of Ct values for clinical samples analysed for the detection of the four targets using the quadruplex rRT-PCR assay are displayed in Figure 3.

The agreement analysis plot of the two assays on positive samples is shown in Figure 4.

In total, 5.4% (5/91) of the positive points for the SARS-CoV-2 ORF1ab gene and N gene were outside the 95% limits of agreement (LoA), while all the positive points of hIAV and hIBV were within the 95% LoA. Within the 95% LoA, the maximum value of the Ct ratio of the two assays for the SARS-CoV-2 ORF1ab gene was 1.13, and the minimum value was 1, whereas the maximum values of the Ct ratio of the two assays for the SARS-CoV-2 N gene, hIAV and hIBV were 1.1, and the minimum values were 1. This result means that

Table 3
Summary of limit of detection results.

	Lower limit of 95% detection (copies/μL)							
	Singleplex rRT-PCR				Quadruplex rRT-PCR			
	ORF1ab gene	N gene	hIAV	hIBV	ORF1ab gene	N gene	hIAV	hIBV
RNA plasmid	36.98	33.58	41.06	44	49.96	47.56	73.14	55.20
Nucleic acid extract	81.10	59.44	76.16	70.26	100.82	100.4	119.74	114.65

rRT-PCR, real-time reverse transcription polymerase chain reaction.

Table 4
Summary of specificity results.

No.	Strain	Origin	Identified result	Result from this study
1	Human coronavirus 229E (*n* = 6)	NBITHC	+ (*n* = 6)	- (*n* = 6)
2	Human coronavirus OC43 (*n* = 4)	NBITHC	+ (*n* = 4)	- (*n* = 4)
3	Human coronavirus HKU1 (*n* = 3)	NBITHC	+ (*n* = 3)	- (*n* = 3)
4	Human coronavirus NL63 (*n* = 3)	NBITHC	+ (*n* = 3)	- (*n* = 3)
5	Parainfluenza virus 1 (*n* = 2)	NBITHC	+ (*n* = 2)	- (*n* = 2)
6	Parainfluenza virus 2 (*n* = 2)	NBITHC	+ (*n* = 2)	- (*n* = 2)
7	Parainfluenza virus 3 (*n* = 1)	NBITHC	+ (*n* = 1)	- (*n* = 1)
9	Human metapneumovirus (*n* = 3)	NBITHC	+ (*n* = 3)	- (*n* = 3)
10	Adenovirus 55 (*n* = 8)	NBITHC	+ (*n* = 8)	- (*n* = 8)
11	Respiratory syncytial virus A (*n* = 3)	NBITHC	+ (*n* = 3)	- (*n* = 3)
12	Respiratory syncytial virus B (*n* = 2)	NBITHC	+ (*n* = 2)	- (*n* = 2)
13	Rhinovirus (*n* = 8)	NBITHC	+ (*n* = 8)	- (*n* = 8)
14	Human bocavirus (*n* = 4)	NBITHC	+ (*n* = 4)	- (*n* = 4)
15	*Mycoplasma pneumoniae* (*n* = 2)	Ningbo CDC	+ (*n* = 2)	- (*n* = 2)
16	*Chlamydia pneumoniae* (*n* = 3)	Ningbo CDC	+ (*n* = 3)	- (*n* = 3)
17	*Legionella pneumonia* (*n* = 2)	Ningbo CDC	+ (*n* = 2)	- (*n* = 2)
18	*Bordetella pertussis* (*n* = 1)	Ningbo CDC	+ (*n* = 1)	- (*n* = 1)
19	*Klebsiella pneumoniae* (*n* = 5)	Ningbo CDC	+ (*n* = 5)	- (*n* = 5)
20	*Mycobacterium tuberculosis* (*n* = 1)	Ningbo CDC	+ (*n* = 1)	- (*n* = 1)
21	SARS-CoV (pseudo) (*n* = 1)	NCCL	+ (*n* = 1)	- (*n* = 1)
22	MERS-CoV (*n* = 3)	QCMD	+ (*n* = 3)	- (*n* = 3)
23	SARS-CoV-2 (*n* = 1)	NCCL	+ (*n* = 1)	+ (*n* = 1)
24	(H1N1) pdm09 virus (*n* = 18)	NBITHC	+ (*n* = 18)	+ (*n* = 18)
25	Influenza A virus (H3N2) (*n* = 21)	NBITHC	+ (*n* = 21)	+ (*n* = 21)
26	Influenza A virus (H7N9) (*n* = 1)	Ningbo CDC	+ (*n* = 1)	+ (*n* = 1)
27	Influenza A virus (H5N1) (*n* = 1)	Ningbo CDC	+ (*n* = 1)	+ (*n* = 1)
28	Influenza B virus Yamagata lineage (*n* = 6)	Ningbo CDC	+ (*n* = 6)	+ (*n* = 6)
29	Influenza B virus Victoria lineage (*n* = 9)	Ningbo CDC	+ (*n* = 9)	+ (*n* = 9)

NBITHC, Ningbo International Travel Healthcare Centre; CDC, Centre for Disease Control and Prevention; NCCL, National Centre for Clinical Laboratories; QCMD, Quality Control for Molecular Diagnostics; +, positive result; -, negative result.

Table 5
Summary of evaluation results of clinical samples.

Target	No. of samples with results for quadruplex rRT-PCR *vs* singleplex rRT-PCR				Concordance (%)	Sensitivity		Specificity	
	+/+	+/-	-/+	-/-		TP/(TP + FN)	%	TN/(TN + FP)	%
ORF1ab	88	0	3	221	99	88/91	96.7	221/221	100
N	90	1	0	221	99.6	91/91	100	221/221	100
hIAV	60	0	0	252	100	60/60	100	252/252	100
hIBV	50	0	0	262	100	50/50	100	262/262	100

rRT-PCR, real-time reverse transcription polymerase chain reaction; TP, true positive; FN, false negative; TN, true negative; FP, false positive.

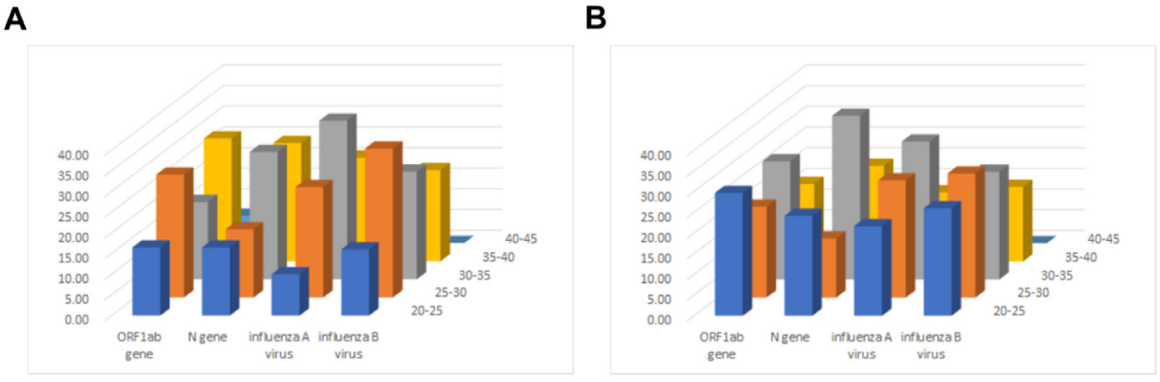

Figure 3. Distribution frequencies of cycle threshold values for positive clinical samples analysed for detection of the ORF1ab gene, N gene, human influenza A virus (hIAV) and human influenza B virus (hIBV) using the quadruplex and singleplex real-time reverse transcription polymerase chain reaction (rRT-PCR) assays. (A) Results for the ORF1ab gene, N gene, hIAV and hIBV by quadruplex rRT-PCR assay. (B) Results for the ORF1ab gene, N gene, hIAV and hIBV by singleplex rRT-PCR assays.

the Ct values of the two assays for the SARS-CoV-2 ORF1ab gene differed by up to 13%, while there was no obvious difference between the Ct values of the two assays for the SARS-CoV-2 N gene, influenza A virus and influenza B virus ($p < 0.05$).

Discussion

A rapid quadruplex rRT-PCR assay for simultaneous detection and differentiation of SARS-CoV-2, hIAV and hIBV in one tube was

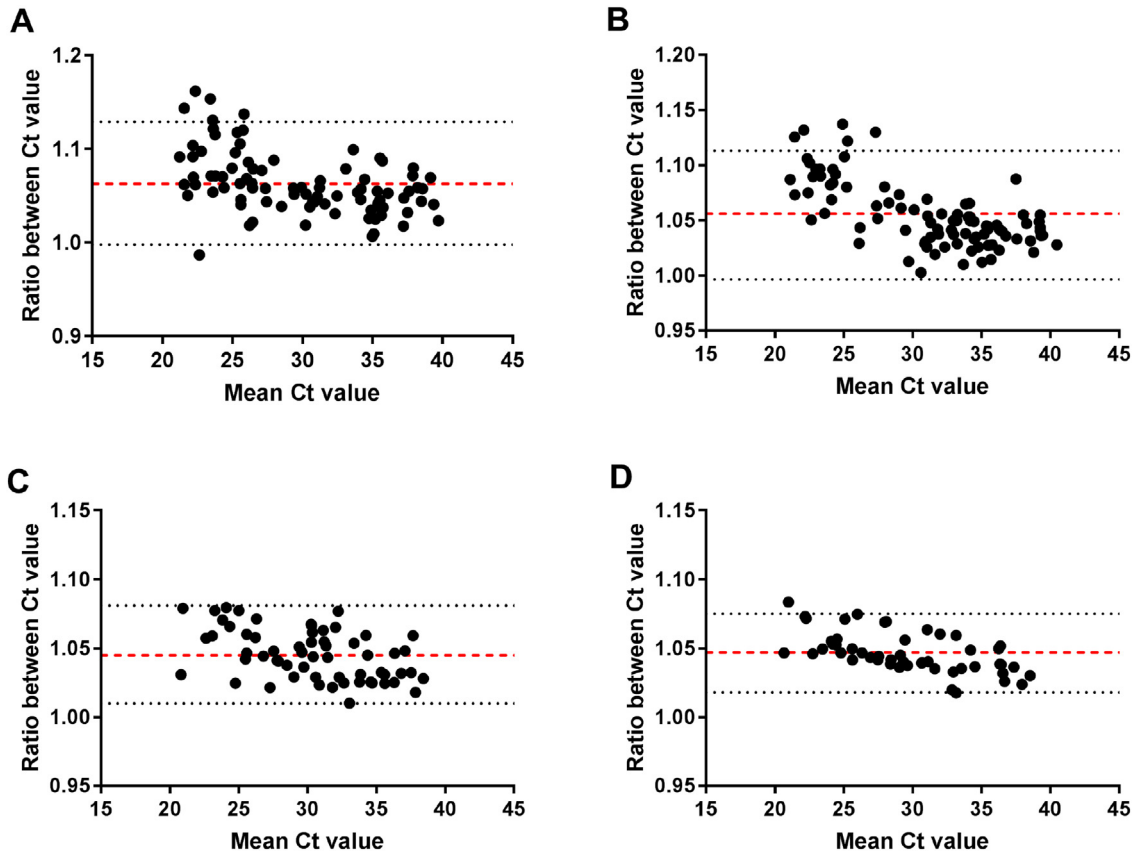

Figure 4. Summary of agreement analysis plots of clinical samples for the quadruplex and singleplex real-time reverse transcription polymerase chain reaction (rRT-PCR) assays by the Bland–Altman ratio method. (A) Agreement analysis plot for the quadruplex and singleplex rRT-PCR assays for the ORF1ab gene. (B) Agreement analysis plot for the quadruplex and singleplex rRT-PCR assays for the N gene. (C) Agreement analysis plot for the quadruplex and singleplex rRT-PCR assays for human influenza A virus. (D) Agreement analysis plot for the quadruplex and singleplex rRT-PCR assays for human influenza B virus. Ct, cycle threshold.

developed. This assay was established by screening primers and probes, optimizing the system, and then validating the assay in accordance with the analytical procedures and methods validation for drugs and biologics recommended by the US Food and Drug Administration. The optimized quadruplex rRT-PCR assay reported here can detect the N gene and ORF1ab gene of SARS-CoV-2, hIAV and hIBV specifically and sensitively. More importantly, this assay can not only sensitively detect SARS-CoV-2, but can also precisely distinguish influenza virus from SARS-CoV-2, especially for the recently reported co-infections of SARS-CoV-2 and hIAV or human metapneumovirus (Kim et al., 2020; Touzard-Romo et al., 2020; Wu et al., 2020). In comparison with the singleplex rRT-PCR assay, the quadruplex rRT-PCR assay decreased sample turnaround time at least three-fold by reducing the number of separate tests.

Moreover, with the aim of detecting all SARS-CoV-2, hIAV and hIBV in a 96-well fluorescent PCR detection system, this quadruplex rRT-PCR assay can analyse at least 94 samples at the same time, whereas the singleplex rRT-PCR detection assay can only analyse up to 30 samples simultaneously.

The quadruplex rRT-PCR assay was highly specific without any cross-reactivity, with non-specific amplification of other respiratory viruses and specific amplification of different subtypes of influenza A and B viruses. Due to the presence of four sets of primers and probes in one tube, and the formation of primer or primer/probe dimers, the amplification efficiency of the four targets of the quadruplex rRT-PCR assay is slightly lower than that of the singleplex rRT-PCR assay, resulting in the sensitivity of the four targets of the quadruplex rRT-PCR assay being no more than two-fold lower than that of the singleplex rRT-PCR assay; this was considered acceptable for clinical diagnosis. Inter- and intra-assay variation exhibited excellent repeatability, which indicated that this assay can be used effectively for clinical performance. Moreover, the clinical performance of the quadruplex rRT-PCR assay was validated on a wide range of samples with diverse types, including a high number of positive samples. This assay is consistent with the singleplex rRT-PCR assays and the original sample results. For the four inconsistent samples, it may be that the viral load was too low to keep discordance with the first result, but in subsequent retests, the results of the two assays remained consistent. In conclusion, to the authors' knowledge, this is the first study to report the development of a quadruplex rRT-PCR assay for the detection of two SARS-CoV-2 genes, hIAV and hIBV with perfect clinical performance. In comparison with cell culture and singleplex rRT-PCR assays, this quadruplex rRT-PCR assay can reduce both cost and time considerably. In addition, this quadruplex rRT-PCR assay has excellent specificity, sensitivity and accuracy for the detection of SARS-CoV-2, hIAV and hIBV. Fast and accurate differential diagnosis of SARS-CoV-2, hIAV and hIBV can not only facilitate early intervention in epidemics with similar clinical symptoms, such as pneumonia, but can also confirm SARS-CoV-2 quickly. This assay could play an important role in curbing the COVID-19 epidemic.

Conflict of interest

None declared.

Funding source

This study was supported by the National Key R & D Programme (<GN1>2</GN1>018ZX10101003-002-002) and the Natural Science Foundation of Ningbo (2017C50034).

Ethical approval

The Ethics Committee of Ningbo ITHC approved all experimental procedures. All experiments were conducted in accordance with approved guidelines.

References

Broeders S, Huber I, Grohmann L, et al. Guidelines for validation of qualitative real-time PCR methods. Trends Food Sci Technol 2014;37:115–26.
Coiras MT, Pérez-Breña P, García ML, Casas I. Simultaneous detection of influenza A, B, and C viruses, respiratory syncytial virus, and adenoviruses in clinical samples by multiplex reverse transcription nested-PCR assay. J Med Virol 2003;69:132–44.
Fang SS, Li JX, Cheng XN, et al. Simultaneous detection of influenza virus type B and hIAV subtypes H1N1, H3N2, and H5N1 using multiplex real-time RT-PCR. Appl Microbiol Biotechnol 2011;90:1463–70.
Hindiyeh M, Levy V, Azar R, et al. Evaluation of a multiplex real-time reverse transcriptase PCR assay for detection and differentiation of influenza viruses A and B during the 2001–2002 influenza season in Israel. J Clin Microbiol. 2005;43:589–95.
Huang C, Wang Y, Li X, et al. Clinical features of patients infected with 2019 novel coronavirus in Wuhan, China. Lancet 2020;395:497–506.
Kim D, Quinn J, Pinsky B, Shah NH, Brown I. Rates of co-infection between SARS-CoV-2 and other respiratory pathogens. JAMA 2020;323:2085–6.
Lai CC, Liu YH, Wang CY, et al. Asymptomatic carrier state, acute respiratory disease, and pneumonia due to severe acute respiratory syndrome coronavirus 2 (SARS-CoV-2): facts and myths. J Microbiol Immunol Infect 2020;53:404–12.
Okela P, Piiparinen H, Luiro K, Lappalainen M. Detection of human metapneumovirus and respiratory syncytial virus by duplex real-time RT-PCR assay in comparison with direct fluorescent assay. Clin Microbiol Infect 2010;16:1568–73.
Touzard-Romo F, Tapé C, Lonks JR. Co-infection with SARS-CoV-2 and human metapneumovirus. R I Med J 2020;103:75–6.
Valencia DN. Brief review on COVID-19: the 2020 pandemic caused by SARS-CoV-2. Cureus 2020;12:e7386.
Wang Y, Wang Y, Chen Y, Qin Q. Unique epidemiological and clinical features of the emerging 2019 novel coronavirus pneumonia (COVID-19) implicate special control measures. J Med Virol 2020;92:568–76.
Wilkesmann A, Schildgen O, Eis-Hubinger AM, et al. Human metapneumovirus infections cause similar symptoms and clinical severity as respiratory syncytial virus infections. Eur J Pediatr 2006;165:467–75.
Williams JV, Harris PA, Tollefson SJ, et al. Human metapneumovirus and lower respiratory tract disease in otherwise healthy infants and children. N Engl J Med 2004;350:443–50.
Wu Xj, Cai Y, Huang X, et al. Co-infection with SARS-CoV-2 and hIAV in patient with pneumonia, China. Emerg Infect Dis 2020;26:1324–6.
Zheng J. SARS-CoV-2: an emerging coronavirus that causes a global threat. Int J Biol Sci 2020;16:1678–85.